SOLPENCO vs Observations

A first analysis

A. Aran[1], B. Sanahuja[1,2], D. Lario[3]

(1) Departament d'Astronomia i Meteorologia. Universitat de Barcelona. Spain

(2) Institut de Ciències del Cosmos, UB. Barcelona. Spain

(3) Applied Physics Laboratory. The Johns Hopkins University, Maryland. USA

Abstract

Current models for the prediction of the fluxes and fluences of solar energetic particle (SEP) events are useful for integral mission durations. Nevertheless, a major drawback of these models is that they do not provide predictions for individual SEP events. We have developed a code that is a first attempt to forecast proton fluxes and the upstream fluences of individual SEP events associated to CME-driven interplanetary shock waves. The **SOLPENCO** code comprises a variety of SEP scenarios, including solar longitudes of the parent solar activity ranging from E75 to W90 for observers located at 1.0 AU and 0.4 AU, and for proton energies between 0.125 MeV and 64 MeV.

We have compared the predicted duration and the peak flux for several proton energies with those of a set of gradual SEP events observed at 1.0 AU from 1998 to 2001. We analyze the results of this validation regarding to the heliolongitude of the SEP event and the transit time of the associated shock, as well as the particle energy. We discuss the limitations of the present version of **SOLPENCO**. We draw conclusions about the improvements to be made in order to provide an operative tool for SEP events forecasting, based on physical models.

Introduction: SOLPENCO

Existing codes for particle flux or fluence forecasting are unable to reproduce the order –of -magnitude deviation of the observed flux from prediction. The main responsible of such situation is the failure of including the effects of interplanetary shocks; operational codes were developed under the paradigm that particle acceleration occurs only at the site of the associated flare event (usually the flare site). This failure and the scarce number of proton flux observations out of 1 AU, are responsible of our poor knowledge of the radial variations of SEP fluxes. Frequently, in many applications, a simple inverse square (or cubic) law is assumed. Therefore, a more complete physical approach in modeling the solar particle generation and propagation in interplanetary space is required, and this approach must be translated into an operational code.

We have been developing a first version of an engineering tool that takes into account the contribution of shock -accelerated protons in the flux of gradual SEP events, in the upstream part of the shock. The main features of this code, named **SOLPENCO** (from **Sol**ar **P**article **En**gineering **Co**de), can be found in Aran et al. (2005b and c).

SOLPENCO is based on:

Shock-plus-Particle Propagation Model
(D. Lario, B. Sanahuja and A. M. Heras, 1998)

2-1/2 D MHD model

(Wu et al., 1983)

Main inputs for the initial shock pulsation:
the initial speed, v_s

Main outputs:

- COBPOINT's location
- MHD variables (VR, BR and θ_{Bn}) at the COBPOINT

VR: the downstream/upstream normalized velocity ratio,
VR = $V_r(d)/V_r(u)$ -1

Proton propagation model

(Lario, 1997; Lario et al., 1998)
Using a focused-diffusion transport equation + solar wind convection + adiabatic deceleration

Main parameters:

- ✓ **Q** (cm^{-6} s^3 s^{-1}), **the injection rate of shock-accelerated particles at the COBPOINT**
- ✓ $\lambda_{\parallel}$, **proton mean free path**

Main outputs:

- **Proton differential flux** at several energies
- **First order anisotropy**

SOLPENCO provides:

Rapid (< 1 minute) predictions of the proton flux and upstream fluence profiles, as well as the transit time and speed of the associated shock for a large set of gradual SEP events characterized by the following parameters (to be chosen by the user):

- **10 energy channels**

E (MeV)	0.125	0.250	**0.500**	1.000	2.000	4.000	8.000	16.000	32.000	64.000
Emin	0.088	0.177	0.354	0.707	1.414	2.828	5.657	11.314	22.627	45.255
Emax	0.177	0.354	0.707	1.414	2.828	5.657	11.314	22.627	45.255	90.510

for 896 possible interplanetary scenarios defined by:

- **8 shocks** (750, 900, 1050, 1200, 1350, 1500, 1650 and 1800 km/s)
- **14 observers** (W90, W75, W60, W45, W30, W22.5, W15, W00, E15, E22.5, E30, E45, E60 and E75)
- **4 particle transport conditions** (mean free path, λ at 0.5 MeV: 0.2 or 0. 8 AU; and presence or absence of a turbulent foreshock)
- **at 1.0 AU and at 0.4 AU.**

The parameters that define these solar-interplanetary scenarios haven been chosen from the SEP events we have already modeled or from the literature, assuming "reasonable average" conditions.

- To synthesize the flux profiles, we assume that the injection rate of shock-accelerated particles at the cobpoint, Q, is given by:

$$\log Q(t, E) = \log Q_0(E) + k\ VR\ (t),$$

where we have adopted **k = 0.5**

- The injection rate is scaled with the energy as a power-law:

$$Q_0\ (E) = C\ E^{-\gamma}$$

with the spectral index γ **= 2 for E < 2 MeV,** and
= 3 for E ≥ 2 MeV.

- The adopted scaling factor corresponds to the value of the 0.5 MeV proton flux arrival of the 12 - 15 September 2000 SEP event, using data from the ACE/EPAM instrument (for a description of this event, see Aran et al., 2005a).

OBSERVATIONAL DATA AND EVENT SELECTION

To compare the fluxes at the energies provided by SOLPENCO with observations, we have used low energy (< 5 MeV) particle data from the LEMS telescope of the ACE/EPAM instrument, with a time resolution of 96s (Gold et al., 1998). For higher energies we have used 330s-averaged data provided by the PET telescope of the IMP8/CPME instrument (Sarris et al., 1976). The 10 energy channels are:

E (MeV)	0.150	0.250	0.424	0.789	1.419	3.020	8.30	19.4	34.6	67.9
Emin	0.115	0.195	0.310	0.587	1.060	1.900	4.60	15.0	25.0	48.0
Emax	0.195	0.321	0.580	1.060	1.900	4.800	15.0	25.0	48.0	96.0

Selection of the SEP events

We have identified the solar origin of 135 interplanetary shocks associated with proton events (SEP events) between January 1998 and October 2001; the energy range investigated extends from 47 keV to 440 MeV.

From this set of SEP events, we have selected those events that: **(1) the association between the shock and a parent solar activity can be reasonably well established; (2) they show a remarkable increase of the flux profiles for E < 96 MeV; and (3) the event is not riding the downstream part of a preceding event** (i.e., the particle background is small). Finally, we choose 17 events, their main features are shown in **Table 1**.

Table1: List of the shock and associated solar origin of the studied SEP events

			IP Shock		Solar Origin								
No.	Year	Doy	Date (mm/dd)	Time at ACE (UT)	CME Date (mm/dd)	Time (UT)	V_{CME} (km/s)	Type	Peak Flare (Xray/H_α)	Onset Time	H_α Location	Reference	Computed initial shock speeds (km/s)
1	1998	113	04/23	17:28	04/20	10:07	1863	H	M1.4	09:38	S43 W90	1,2	1249
2	1998	238	08/26	06:21	08/24	Data Gap			X1.0/3B	21:48	N35 E09	3,4	1399
3	1998	267	09/24	23:13	09/23	Data Gap			M7.1/3B	06:44	N18 E09	4	1136
4	1998	275	10/02	06:53	09/30	Data Gap			M2.8/2N	14:02	N23 W81	4	2248
5	2000	160	06/08	08:41	06/06	15:54	1119	H	X2.3/3B	14:58	N20 E18	1,5	1131
6	2000	197	07/15	14:15	07/14	10:54	1640	H	X5.7/3B	10:03	N22 W07	6	1615
7	2000	259	09/15	04:00	09/12	11:54	1550	H	M1.0/2N	11:31	S17 W09	1,7,8	740
8	2000	302	10/28	09:08	10/25	08:26	770	H	C4.0	08:45	N17 W50	9	781
9	2000	302	10/28	09:08	10/25	08:26	770	H	C4.0	08:45	N17 W90	5,10	1394
10	2000	315	11/10	06:04	11/8	23:06	1738	P	M7.4/1N	22:42	N10 W75	6, 11	2584
11	2001	023	01/23	10:06	01/20	21:30	1507	H	M7.7/2B	21:06	S07 E46	5,12	871
12	2001	031	01/31	07:22	01/28	15:54	916	P	M1.5/1N	15:40	S04 W59	1,12	1007
13	2001	090	03/31	00:23	03/29	10:26	942	H	X1.7/2N	09:57	N16 W12	13,14	1222
14	2001	094	04/04	14:23	04/02	22:06	2505	P	X20/?	21:32	N17 W78	6	2102
15	2001	101	04/11	15:28	04/10	05:30	2411	H	X2.3/3B	05:06	S23 W09	6,13,14	1348
16	2001	108	04/18	00:04	04/15	14:06	1199	P	X14.4/2B	13:19	S20 W85	2,6,9	1566
17	2001	268	09/25	20:02	09/24	10:30	2402	H	X2.6/2B	09:32	S16 E23	10	1387
18	2001	294	10/21	16:12	10/19	16:50	901	H	X1.6/2B	16:13	N15 W29	14,15	1053
19	2001	294	10/21	16:12	10/19	01:17	558	P	X1.6/2B	00:47	N16 W18	16,17	751

1, Gopalswamy et al. (2004); 2,Tylka et al. (2005); 3, Bale et al. (1999); 4, Lario et al. (2000); 5,Cane and Richardson (2003); 6, Lario et al. (2004a); 7, Aran et al. (2005a); 8, SGD679; 9, Kahler (2005); 10, Lario et al. (2003); 11, Nitta et al (2003); 12, Cane et al. (2002); 13, Sun et al. (2002); 14, Manoharan et al. (2004); 15, Lario et al. (2004b); 16, SGD692; 17, url1

Note that events 8 and 9 (as well as 18 and 19) are the same SEP events but with different solar origins

Predicting the time of shock arrival

Figure 1 shows the difference (in minutes) between the observed transit time of the shock and the value predicted by SOLPENCO, for each event of Table 1, as a function of the initial speed of the shock.

Vertical dashed lines indicate the slowest (750 km s^{-1}) and highest (1800 km s^{-1}) initial speeds considered in SOLPENCO. Blank symbols mark those events out of this range. For them the time is expressed in hours. Each event is also classified by the heliolongitude of the associated solar activity:

7 western events (diamonds), **9 central meridian events** (circles) and **1 eastern event** (triangle).

The transit time of the event is well fitted for all the events with initial velocities within the range of the code.

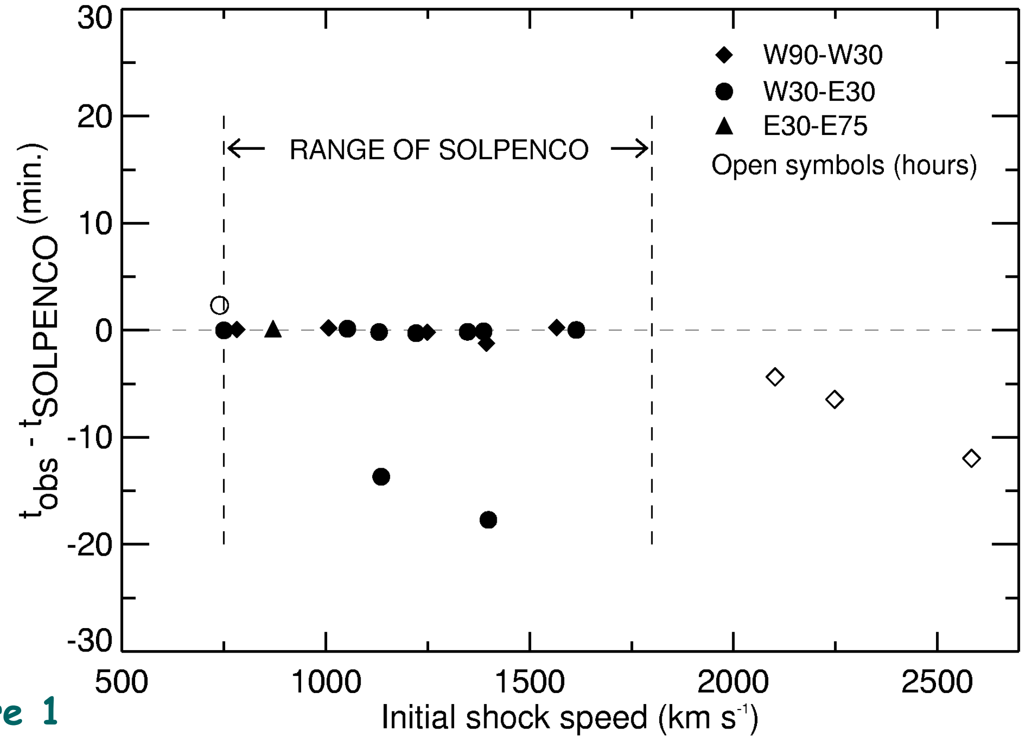

Figure 1

Predicting the peak fluxes (I). Examples

- A western event (W90-W30): 30 – 2 October 1998, #4

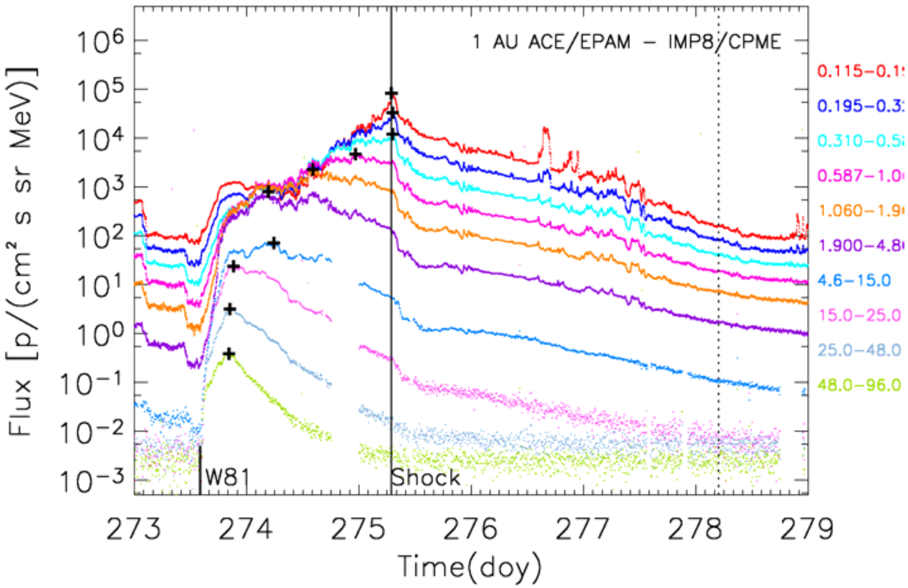

Figure 2#4. Proton differential flux profiles for several energy channels (color coded). Black crosses mark the location of the peak flux for each energy.

Vertical solid line indicates the time of shock arrival and the short vertical bar the time of the associated solar activity (also indicated).

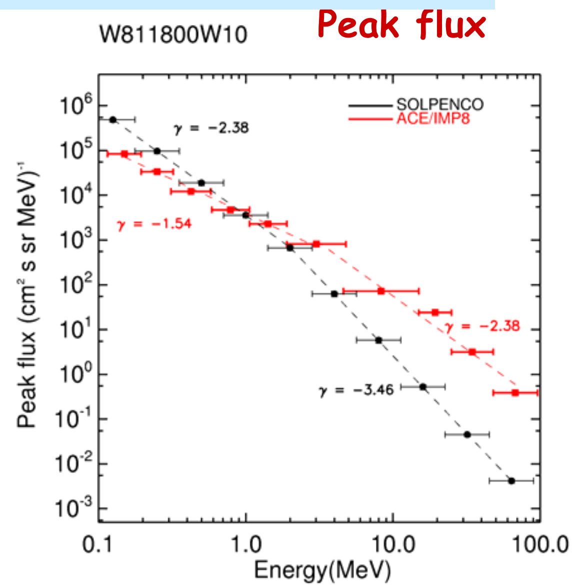

Figure 3#4. Spectrum of the observed (red squares) and predicted (black circles) peak fluxes.

Horizontal bars denote the energy range covered by each channel. SOLPENCO's values displayed are the average value for the four transport conditions. The spectral index at low and high energies is also plotted.

All the analyzed western events present the peak fluxes above 4 MeV short after the onset of the events (from hours to one day) . This feature cannot be reproduced by the present version of **SOLPENCO** (see the discussion in the conclusions) where for only 40 western scenarios (E ≥ 32 MeV) of the database the peak flux appears shortly after the onset.

The predicted values at different energies fit much better the observations at the shock arrival, as can be seen in Figure 4 .

Flux at shock arrival

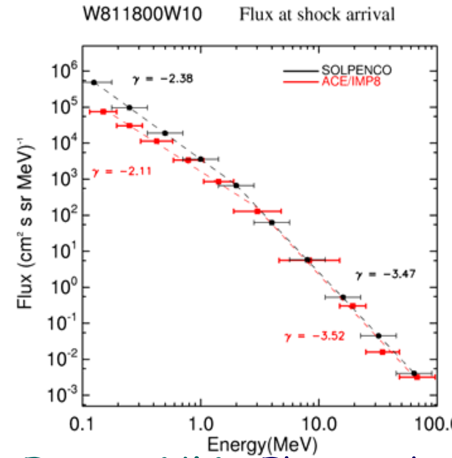

Figure 4#4. Flux at the shock arrival (see Fig. 3)

- A western event (W90-W30): 2 – 4 April 2001, #14

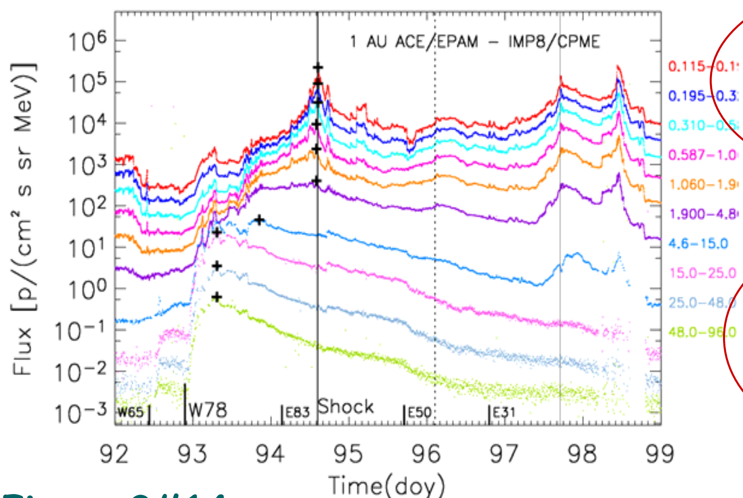

Figure 2#14

The peak flux is fitted well at low energies

But at high energies it shows the same behavior as #4

Peak flux

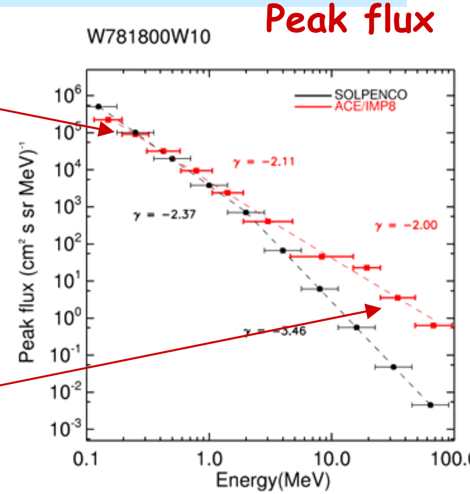

Figure 3#14

- A central meridian event (W30 –E30): 6 – 8 June 2000, #5

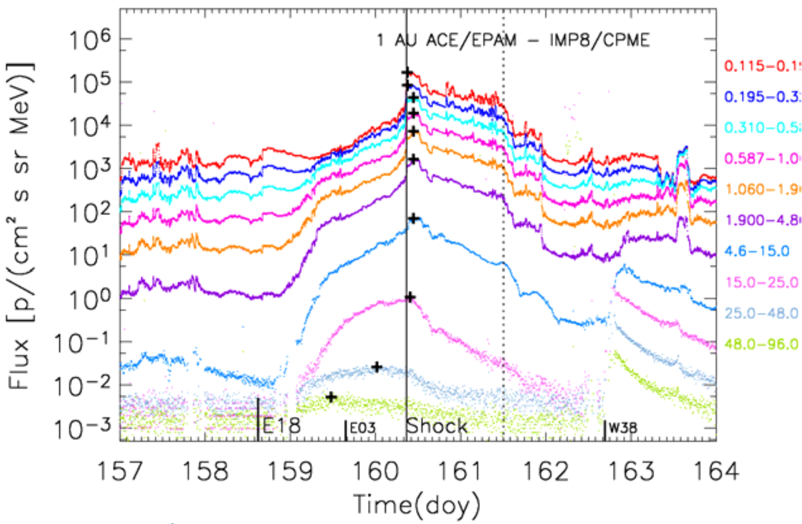

Figure 2#5

Figure 3#5

Peak flux

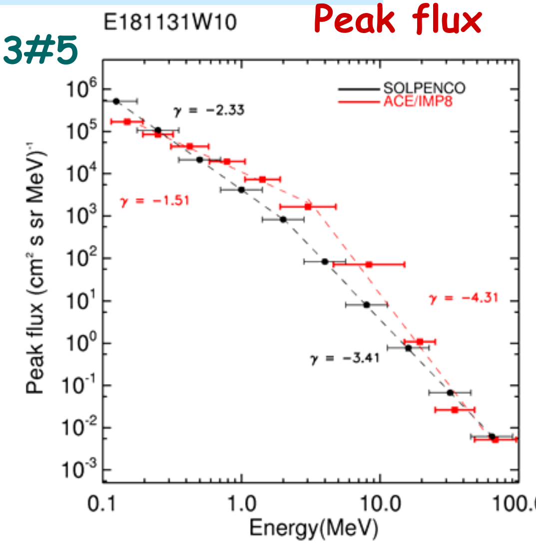

Figure 4#5

Flux at shock arrival

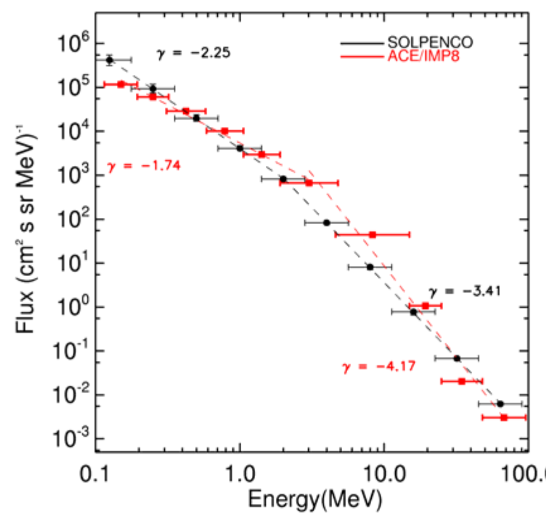

Example of an eastern central meridian event where the peak flux is usually found shortly after the shock passage. The code cannot predict accurately the peak flux value for the channels with the peak downstream. after the shock (Figure 3). But it works for the remaining energy channels, and it is quite good.

The differences found between the observed and predicted values reduce when comparing the values at the time of shock arrival (Figure 4).

But…

- A central meridian event (W30 –E30): 19 – 21 October 2001, #18 -19

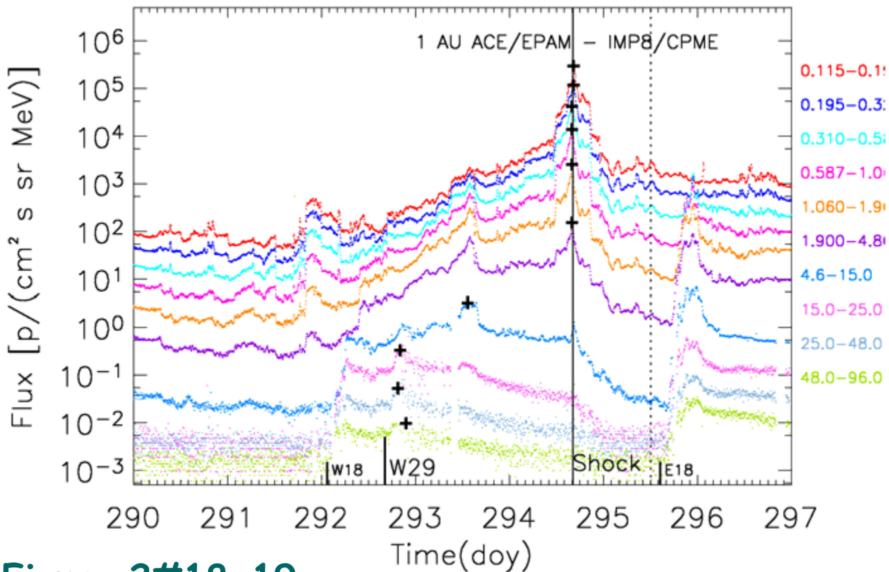

Figure 2#18-19

Peak flux

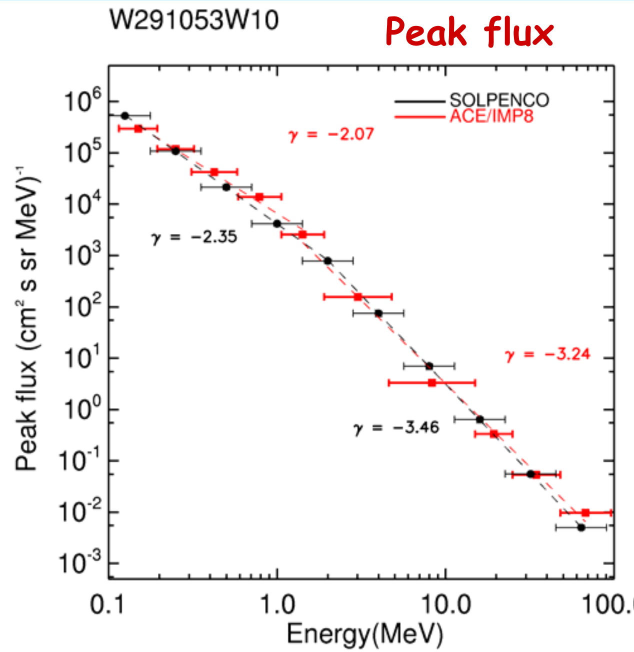

Figure 3 #18-19

This event has two possible solar origins. The solar event at W18, that dominates the evolution of the flux profiles at low energies, and the event at W29, that seems to dominate the time-profile of the four high energy channels. Furthermore, the time of the peak flux from 4.6 to 96 MeV is near the onset of the SEP event, so the peak flux time is neither well defined nor predicted but… the fit is perfect (!!?), see Figure 3.

"Natura mirabilia facit"

Predicting the peak fluxes (II).

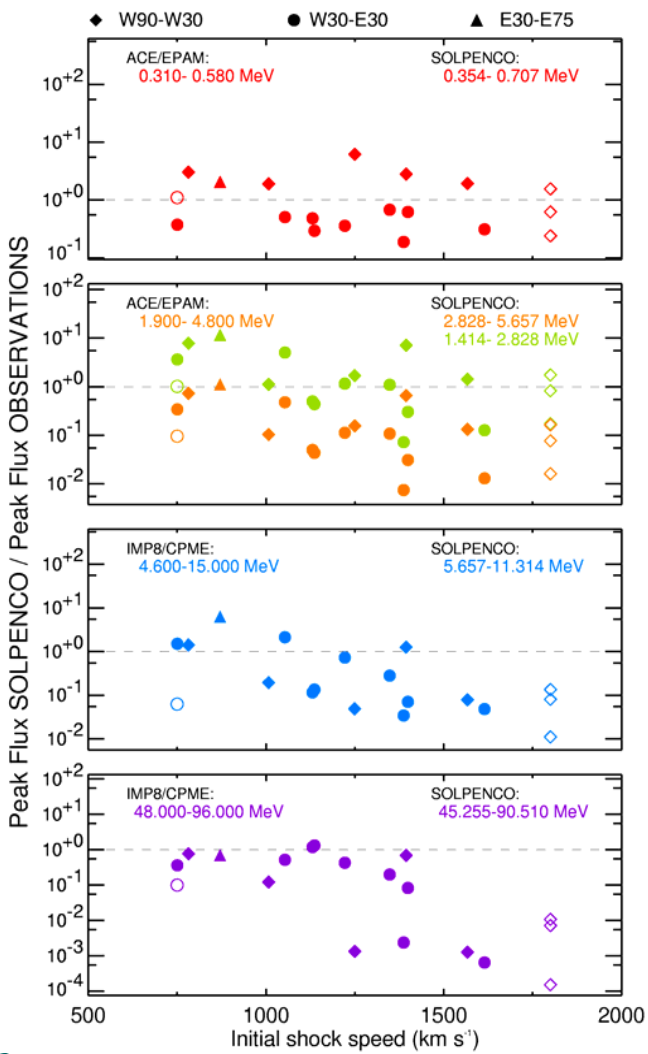

Figure 5

- For each event and for any energy, we have calculated the ratio between the synthetic peak flux value and the observed value. Figure 5 shows these ratios for four ACE or IMP energy channels, from low (~0.4 MeV, top panel) to high energy (~67 MeV, bottom panel).

- The peak flux predictions fit much better with observations at low than at high energy. The worst cases are: (i) the extreme western (>W75) events displaying an intense high energy flux at the onset, (ii) the Bastille event (W07, 1615 km s^{-1}) and (iii) a strong eastern-CM event #17 (E23, 1387 km s^{-1}).

- Second panel from the top compares the peak fluxes observed by the 1.9-4.8 MeV energy channel, with the synthetic fluxes derived at 2 and 4 MeV, respectively. It is clear that the 2 MeV-peak fluxes fit much better than the corresponding values at 4 MeV. Then, the point is: *Do we have to compare the observed peak flux for a given energy channel with the synthetic value computed for the mean energy of the channel (as usually done) or with the peak flux computed for the minimum energy of the channel, instead?*

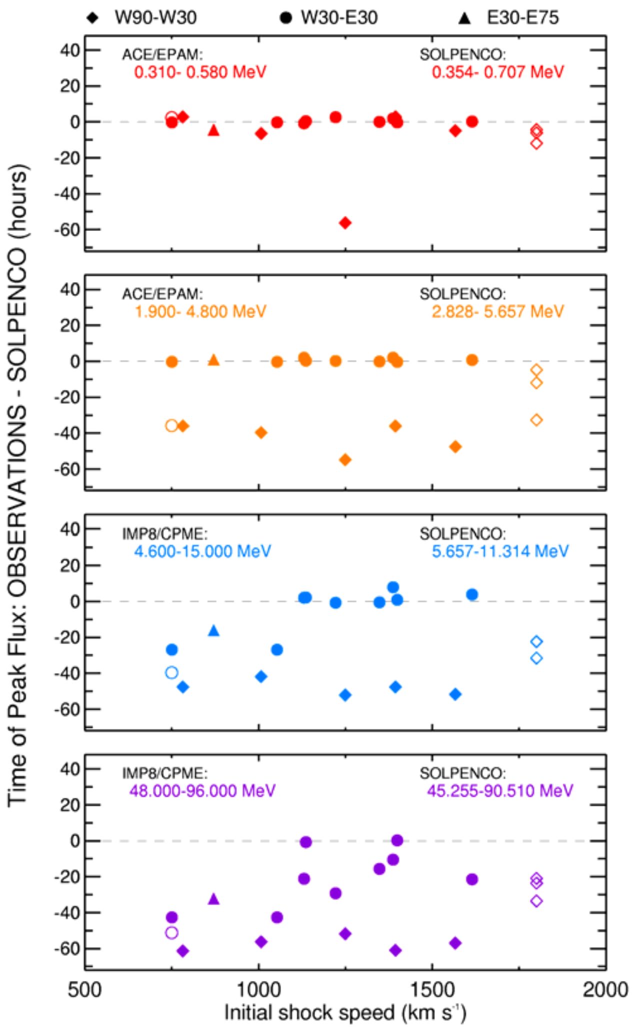

Figure 6

We have analyzed in detail the difference between the observed and the predicted time of the peak flux, for each event (Figure 6, same energies than in figure 5).

- At low energy (~0.4 MeV, top panel), the prediction of the time occurrence of the peak flux is fine. There is one exception, the event #1, (W90, 1249 km s^{-1}).
- At ~3 MeV (second panel), the predictions for Central meridian events are good, but western events can show differences as large as 50 hours.
- At ~8 MeV (third panel), only the fast central meridian events are correctly predicted on time.
- Finally, for the highest energy channel, ~67 MeV, the fits show important differences in many cases (larger than half a day in several cases).

The main reason of such increasing deviations is that flux profiles are increasingly dominated by the protons accelerated at the onset of the event, thus closer to solar corona. The inner boundary of the shock-plus-particle model (at 18 $R_{\odot}$) prevents a more accurate modeling of such early injection.

Predicting spectral indices (III).

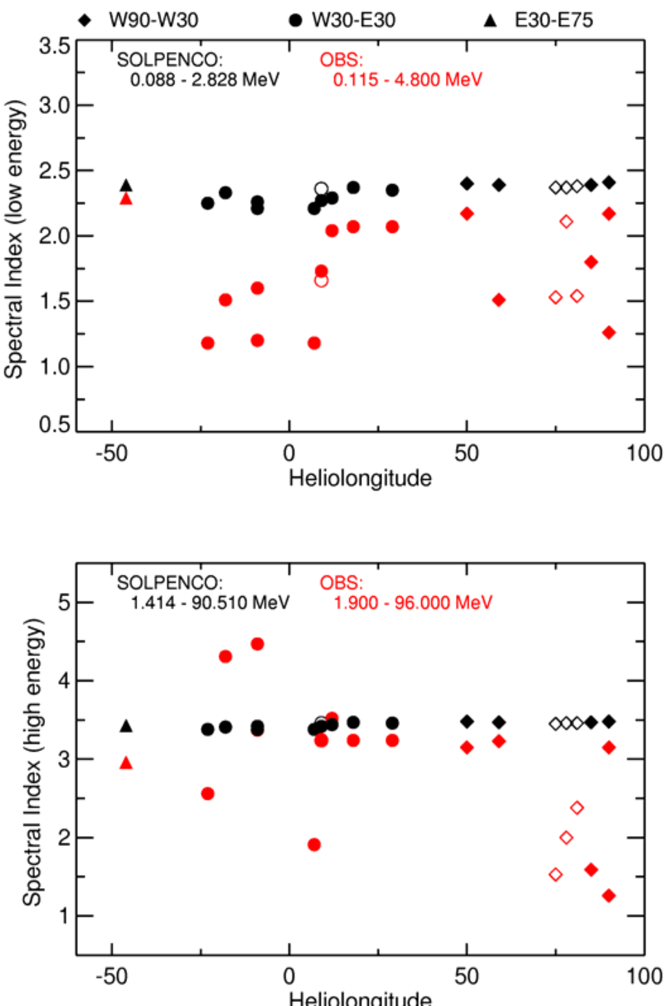

Figure 7

We have compared the values of the spectral index at the peak flux predicted by SOLPENCO (see figures 3), with the corresponding observed value, as function of the heliolongitude of the parent solar activity. Figure 7 show these values at low (< ~4 MeV, top panel) and high (from ~2 MeV to ~67 MeV, bottom panel) energy, for each SEP event between E50 and W90 (binned in three groups). Red and black symbols represent values derived from observations and predictions, respectively.

SOLPENCO produces an almost constant spectral index either at low or at high energy. This is due to the fact that we selected the same spectra for the injection rate of the shock-accelerated protons, independently of the heliolongitude of the event and the initial speed of the shock.

From the studied events it is not possible to derive any significant trend of the spectral index as a function of the heliolongitude, at low energy. At high energy, the events with the highest initial velocities display the softest spectra (that means, a powerful injection).

Discussion and conclusions

We have started the validation of SOLPENCO by comparing part of its outputs with observations, for the strongest SEP events measured at 1 AU by ACE and IMP, for different energies between ~0.1 and ~95 MeV, in the period from January 1998 to October 2001. We have presented a comparative analysis of the predictions of the time of shock arrival, and the values of the maximum proton differential flux intensity ('the peak flux') regarding three factors: the initial velocity of the shock, the heliolongitude of the solar parent activity and the spectral index.

• The **transit times of the events are well fitted** within the range of values of the scenarios provided by SOLPENCO, except for the two E09 events (although the difference is small). This discrepancy can be easily removed by reducing the size of step of heliolongitudes in the database grid.

• The parameters selected to generate the database of SOLPENCO are basically derived from modeling individual SEP events, fitting simultaneously both the proton flux and the first order anisotropy for various (usually ten) energy channels between ~0.1 MeV and ~5 MeV. In several cases SEP modeling extend up to ~50 MeV, but without observational anisotropies to compare with. Therefore, **the number of spectral indices at high energy derived from modeling is still scarce, making difficult to evaluate to which point they are 'representative' values (1**); for example, when choosing the values for the parameter k (Lario, 1997).

Observations (i.e., Cane et al., 1998) show that, **at** high energy, SEP events **display a wide range of spectral indices (2)**, even without taking into consideration their parent solar heliolongitude (or other factors not considered by the shock-plus-particle model). Furthermore, the **energy windows of the high energy channels are too wide (3)** to perform a full reliable comparison. **Facts (1), (2) and (3) combine to make less reliable SOLPENCO predictions at high energies than at low energies.**

- The peak fluxes of the SEP events analyzed are well predicted by SOLPENCO at low energies (< 1-2 MeV). At these energies the main contributor of accelerated particles is the CME-driven shock, hence for, SOLPENCO provides good predictions. As increasing higher energies are considered, the events with a relatively poor magnetic connection at the onset (that is, in average, eastern and central meridian events) the predicted values are still good.

- For well-connected and fast events (western and western-central meridian events), predictions increasingly separate from observations at ~2 MeV. For these events the present version of SOLPENCO is not able to routinely and accurately predict the time and intensity of the peak flux for E > 5 MeV. The reason is two fold: (a) the initial conditions of the MHD code are placed at 18 $R_\odot$, so we are missing the powerful injection of the most energetic particles near the Sun and (b) the code uses a proportional factor between Q and VR (k = 0.5) essentially derived from the modeling at low energies. Thus, **we have to use a MHD code with initial conditions closer to the Sun and -most probably- a higher value of k at high energy, for this type of events** (Aran et al., 2005a)

- To analyze the evolution of the peak flux with the particle energies we have derived the spectral indices by fitting the flux as a power law of the energy. **At low energy (0.1–3 MeV) the predicted spectral index is harder than the observed one**. If we only take into account the analyzed events, **the spectral index adopted to generate the data base should be softer.**

- For **higher energies** (from ~3 to ~95 MeV), **spectral indices are well fitted** by SOLPENCO **for central meridian and western events, with small or medium** (< 1300 km s^{-1}) **initial shock speeds**. The fastest events show a softer spectral index, pointing out a more powerful injection than for the other events. The two eastern-CM events with initial shock speeds about ~1100 km s^{-1} show a spectra harder than that predicted.

We have presented the first analysis of the match between part of SOLPENCO outputs and observations. The number of events analyzed here is still too small to derive any conclusion statistically significant. We have drawn conclusions about the usefulness of SOLPENCO that must be revisited in the future after: **(1) modeling more SEP events, including those that do not show component at high energy** (let's say, E > 50 MeV); (2) **analyzing spectral indices** and other features of flux profiles **at high energies, as a function of the heliolongitude** (and, whenever possible, using the energy channels best suited for space weather – in fact, our- purposes); and (3) **revisiting the way the synthetic flux profiles** at a given energy **are compared with observations.**

Acknowledgements

We acknowledge the financial support of the Ministerio of Educación y Ciencia (Spain) under the projects AYA2001-3304 and AYA2004-03022, as well as partial support from ESA/ESTEC (Contract 14098/99/NL/MM). Partial computational support has been provided by the Centre de Supercomputació de Catalunya (CESCA). We acknowledge the use of ACE/EPAM and IMP8/CPME data and the ACE Service Center for providing proton ACE data. BS acknowledges the support of COST 724 Action.

References

- Aran, A., Sanahuja, B. and Lario, D., Adv. in Space Research, doi:10.1016/j.asr.2005.09.019, 2005a (in press).
- Aran, A., Sanahuja, B. and Lario, D., Adv. in Space Research, doi:10.1016/j.asr.2005.09.019, 2005b (in press).
- Aran, A., Sanahuja, B. and Lario, D., Annales Geophysicae, 23, 1-7, 2005c (in press).
- Bale, S. D., Reiner, M. J., Bougeret, J.-L., et al., Geophys. Res. Letters, 26, 11, 1573-1576, 1999.
- Cane, H. V., and I. G. Richardson, J. Geophys. Res., vol. 108, A4, 1156, doi:10.1029/2002JA009817, 2003.

- Cane, H.V., Erickson, W.C., and Prestage, N.P., J. Geophys. Res., vol. 107, A10, 1315, doi:10.1029/2001JA000320, 2002.
- Cane H.V., Reames D.V., von Rosenvinge T.T., 1988, J. Geophys. Res., 93, 9555
- Gold, R.E., Krimigis, S.M., Hawkins III, S.E., et al., Space Sci. Rev., 86 (1-4), 541, 1998
- Gopalswamy, N., Yashiro, S., Krucker, S. et al., J. Geophys. Res., vol. 109, A12105, doi:10.1029/2004JA010602, 2004.
- Kahler, S. W., Astrophys. J, 628, 1014, 2005
- Lario, D., Livi, S., Roelof, E. C., et al., J. Geophys. Res , 109, A09S02, doi:10.1029/2003JA010107, 2004a
- Lario, D., Decker, R. B., Roelof, E. C., et al., J. Geophys. Res., 109, A01107, doi:10.1029/2003JA010171, 2004
- Lario, D., Roelof, E.C., Decker, R. B., et al., Adv. Space Res., 32, 4, 579-584, 2003
- Lario, D., Marsden, R.G., Sanderson, R.T., et al., J. Geophys. Res., , vol. 105, A8, 18, 251-18, 274, 2000.
- Lario D., Sanahuja B. and Heras A. M., Astrophys. J., 509, 415, 1998
- Lario,D., 1997, PhD. Thesis, Universitat de Barcelona
- Manoharan, P. K., Gopalswamy, N., Yashiro, S., et al., J. Geophys. Res, 109, A06109, doi:10.1029/2003JA010300, 2004.
- Nitta, N., Cliver, E. W., Tylka, A. J., Astrophys. J, 586, L103-L106, 2003
- Sarris, E.T., S.M. Krimigis and T.P. Armstrong, J. Geophys. Res., 81, 2341,1976
- Sun, W., Dryer, M., Fry, C. D., et al., Annales Geophysicae, 20, 937-945, 2002

- Tylka, A. J., Cohen, C. M. S., Dietrich, W. F., et al., Astrophys. J, 625, 474, 2005
- Wu S.T., Dryer M., Han S.M., 1983, Solar Physics., 84, 395
- Solar Geophysical Data Report: SGD692
- url1: Yashiro, S. and Michalek, G., LASCO-CME Catalog: http://cdaw.gsfc.nasa.gov/CME list/